Current Journal of Applied Science and Technology

40(29): 37-50, 2021; Article no.CJAST.74830
ISSN: 2457-1024
(Past name: British Journal of Applied Science & Technology, Past ISSN: 2231-0843, NLM ID: 101664541)

New Theoretical Model of Electric Arc in Circuit Breaker and the Role of Parallel Resistance – The Shunt

S. Bjelić[1], N. Marković[2*], U. Jakšić[3] and F. Marković[4]

[1]Faculty of Technical Sciences, Knjaza Miloša 7, 38220 Kosovska Mitrovica, Kosovo under Resolution 1244, UN, USA.
[2]Kosovo and Metohija Academy of Applied Studies, Department Uroševac – Leposavić, 24 Novembre, 38218 Leposavić, Kosovo under Resolution 1244, UN, USA.
[3]Kosovo and Metohija Academy of Applied Studies, Department Zvečan, Nušićeva 6, 38227 Zvečan, Kosovo under Resolution 1244, UN, USA.
[4]Faculty of Technical Sciences, Knjaza Miloša 7, 38220 Kosovska Mitrovica, Kosovo under Resolution 1244, UN, USA.

Authors' contributions

This work was carried out in collaboration among all authors. Author SB designed the paper and wrote the first version of the paper. Author NM has conducted statistic analysis and simulation in MATLAB program package and made technical preparation of the paper. Authors UJ and FM were responsible for bibliography. All authors read and approved the final manuscript.

Article Information

DOI: 10.9734/CJAST/2021/v40i2931540
Editor(s):
(1) Dr. Chien-Jen Wang, National University of Tainan, China.
Reviewers:
(1) Kuo-Chien , Liao, Chaoyang University, China.
(2) Manu Mitra, University of Bridgeport, USA.
Complete Peer review History: https://www.sdiarticle4.com/review-history/74830

Original Research Article

Received 06 August 2021
Accepted 13 October 2021
Published 23 October 2021

ABSTRACT

Aims: The paper presents a new theoretical model of an electric arc in a circuit breaker with reference to the role of shunt resistance parallel to the electric arc in a circuit breaker switch. One of the goals of the paper is to show the efficiency of using the software package MATLAB Simulink in which the previously derived system of equations is easily implemented in the blocks of the mentioned software package.
Methodology: The discharges in the electric arc determine the potential between the metal contacts of the switch and the structure and shape of the electric arc make it difficult to solve the

**Corresponding author: E-mail: nen.mark74@yahoo.com;*

transient process. The main step in solving the problem is the formation of a theoretical model of the electric circuit from which the current and voltage can be determined, which depend on the parameters of the electric field in the arc. The use of shunts in oil and air switches, due to a number of shortcomings, was not possible, but the disadvantages are overcome if thyristors are used to interrupt the current. The equations and the algorithm for solving the problem are obtained from the parameters of the electric field potential that shape the electric arc and its path. The accuracy of the theoretical model is confirmed by voltage and current diagrams in the adapted MATLAB Simulink software package.

Conclusion: The presented theoretical model and algorithm are universal and can be used for different states in which an electric line can be found. Problems that occur in the analysis of transient processes in an electric circuit where an electric arc occurs can be minimized using different types of simulations. Changing any parameter in the electrical circuit requires a new calculation of the state of the circuit from the very beginning due to the new initial conditions. Analytical methods combined with the simulation method were used in the research of overvoltages, asymmetries and harmonics during the appearance of an electric arc. The MATLAB simulation program had a threefold purpose: to serve the calculation and simulation of quantities that can be obtained by testing or measurement, to establish the original algorithm and to verify the proposed method. Also, this type of simulation can replace the type tests of the electric arc on the switch.

Keywords: Simulation; model; electric arc; transient process; discharge.

1. INTRODUCTION

In an electric arc, thermal processes, unlike electromagnetic processes, are difficult to analyze. For the analysis of electromagnetic processes in an electric arc, existing programs and simulations are modified and new ones are developed to check and verify theoretical models obtained by analytical methods. Static characteristic of electric arc corresponds to the stationary or quasi-stationary state of arc combustion, provided that the resistance is constant, while the dynamic characteristic of the arc is determined by the heat transfer conditions from the arc column. From the measurement of the obtained gradient, $E = f(I_\ell)$ the transient resistance of the arc can be obtained and the process can be simulated in order to avoid the measurement [1,2].

Transient processes in the circuit-breaker arc are affected by commutation and atmospheric overvoltages that can vary widely, with discharges being able to generate overvoltages of the order of several MV [3]. In his book S. Bjelić [4] notes that the discharge phenomenon creates overvoltages on lines, loads and conductive elements, which are described by differential equations. Discharge in these cases (in addition to the influence of overvoltage) acts on the conductor similarly to low frequency current through thermal and electrodynamic effect. In addition to deriving a system of equations that are easily implemented in the blocks of the MATLAB Simulink software package, a simulation with diagrams for comparing the current and voltage of an electric arc in a circuit breaker will be presented.

2. SURVEY OF RELEVANT PAPERS

Dealing with problems that occur in analysis of transient processes in an electric circuit where an electric arc occurs is not a new phenomenon. A large number of researches have been conducted on this topic and a large number of papers have dealt with this issue [2,5-8].

Authors in their research start from an assumption based on the dynamic theory of electric arc defined by the models of M. Kassi and O. Mayr [5,6].

M. Kassi model: In the arc model, the longitudinal electrical conductivity and the dissipated thermal power are constants, while the cross-sectional area of the arc depends on current and time. In steady state, the volt-ampere diagram does not depend on the current density and amounts:

$$P_0 = E^2 / \rho_r \,,\ \vec{E} = \sqrt{\rho_r P_0} \qquad (1)$$

where ρ_r is specific resistence, P_0 power output per unit volume.

O. Mayr model: Assumption is that the radius of arc channel is constant and that the temperature

changes along the radius. Solution for the dynamic volt-ampere characteristic is obtained from the model, and in the equation for resistance the parameters are: thermal time constant T_{arc} and power output P_0 in volume unit [9-11].

The static and dynamic volt-ampere characteristic is important for determining resistance of an arc per unit length $R_l^0 = R_\ell / \ell = V/(\ell \cdot i_\ell) = \vec{E}/\ell$ and it is defined by a voltage gradient $E = grad\vec{V}_l$ [5,6]. For harmonic currents, the arc voltage has a special shape: it initially rises to a maximum $V_{a\,max}$ – the ignition voltage then decreases to a minimum $V_{a\,min}$ and rises again to the quenching voltage V_{ag} . The current is different from a sinusoid; before passing through zero it declines slowly and then rises rapidly. Ignition voltage is affected by processes during the current break (slow change of current around zero value).

In the analysis of arc voltage diagrams V_a , G. Ajerton used equation [12]:

$$V_a = a + b\ell + (c + d\ell)/I_a \tag{2}$$

where a,b,c,d are constant, V_a arc voltage, ℓ arc length, I_a arc current.

From the previous, the equation for the minimum gradient of the arc is derived, which reads:

$$E_a = \partial V_a / \partial \ell = b + d/I \tag{3}$$

Since arc is a combined thermal and electromagnetic process, influence of the volt-ampere characteristic of arc, temperature and pressure on ionization must be taken into account, but Saga, Habedanka equations in the O. Mayr model did not meet prescribed requirements [5,6,8-10,12-14].

In the works of Schiera [14], Burgsdorf [15] and Warington [16], following equations for equivalent resistance were used, which are shown in Table 1.

The notations in the equations are as follows: I – current, ℓ – the length of the lower part of the arc - at the beginning is equal to the distance between the electrodes and increases due to the transverse air currents because the arc has no inertia (thunder in a storm). The exact equation for the arc resistance has not been determined and experiments show that the arc voltage gradient $E = 15$ V/cm for current $I \geq 10^2$ A a little depends on the current and that is why the resistances are calculated by the equations in the table 1 slightly different.

At the end of the review of relevant papers, we conclude that energy transfer is described by differential equations: elliptical for stationary processes (without changes in time and space) and parabolic and hyperbolic for non-stationary processes (changes in time) where the following parameters are determined: E filed strength, D electro-static induction and B magnetic induction ($\vec{B} = rot\vec{A}$, where A is a vector of potential). Maxwell, Poisson and Laplace equations for arc voltage and potential are used for the above processes $\varphi(x,y,z)$, $\Delta(v,\varphi) = 0$ in Decart coordination system:

$$\nabla^2\varphi = \frac{\partial^2\varphi}{\partial x^2} + \frac{\partial^2\varphi}{\partial y^2} + \frac{\partial^2\varphi}{\partial z^2} = 0 \tag{4}$$

where φ is potential of arc and, Δ is Laplas operator.

Equation of Puason and Laplas have one solution with tasked limited conditions:

1. The first line (Dirikle) – on border G value of seeking function is $\varphi = f_1(x,z,y)$ and points of Decart coorrdinates (x,z,y) belog to border G . Condition $\varphi = 0$ is homogeneic contition.
2. The second line (Neiman) – on the border G value of demanded function in normal is $\partial\varphi/\partial n = f_2(x,y,z)$ for coordinate points (x,y,z) . Condition $\partial\varphi/\partial n = 0$ is homogenic condition.
3. The third line – on border G value of demanded function is $\partial\varphi/\partial n + f_3(\varphi) = f_4(x,y,z)$ and points of coordinate (x,y,z) belong to border G . At the domain boundary, conditions can also be specified that contain conditions - first, second and third order.

3. NEW THEORY MODEL OF ELECTRIC ARC

Attached references do not systematize important process parameters in the electric arc

and that is why the authors came up with idea to form a new model that contains a sufficient number of such parameters. Coming up of this idea also arose due to the fact that classical theory of electron motion in an electric arc was exposed to expert criticism. In continuation of this paper, certain corrections were made to this theory, which are given in a new theoretical model that shows a more important part of electrical processes in a modern way. Dependence of the physical and electrical parameters of electric arc is determined by the following equations:

1. Field strength, i.e. scalar potential function between electrodes: $\vec{E} = -grad\varphi$.

2. Continuity is defined by the densities of electronic and ionic currents. If the charge is a particle e, electrone concentration is $\partial n_e / \partial t$ and ions $\partial n_i / \partial t$ then: $div\left(\vec{J}_e + \vec{J}_i\right) = e\left(\partial n_e / \partial t - \partial n_i / \partial t\right)$; where the right - hand side of the equation represents the reduced number of charges in that volume per unit time.

3. Equation of Puason: $div\vec{E} = e\left(n_i - n_e\right)/\varepsilon_0$, where $\varepsilon_0 = 8.85 \cdot 10^{-12}$ [F/m] dielectric constant of air.

4. The expression for the electron/ion current density is defined by Ohm's law ($\vec{J} = \sigma\vec{E}_{out}$) and is a consequence of a foreign field caused by different spatial concentrations of charge:

a) $J_{kn.e} = e \cdot d_e gradn_e$,
$J_e = J_{e.mob} + J_{kn.e} = en_e b_e E + e \cdot d_e gradn_e$

b) $J_{kni} = -d_i gradn_i$,
$J_i = J_{ion.mob.} + J_{kn.i} = en_i b_i E - e \cdot d_i gradn_e$
where d_e electron diffusion coefficient, d_i ion thermal diffusion coefficient.

In the right part of both equations, the first term is determined by the mobility and the second term by the diffusion of particles.

5. Current density continuity $div\vec{J} = -\sigma \cdot div\vec{E} = -\partial\rho / \partial t$ and electrons whose number is equal to the difference of the ionized ones $\partial n_{e.i} / \partial t$ and missing particles in transition $div\vec{J}_e / e$, i.e. $\Delta_e = \left(\partial n_{ei} / \partial t\right) - div\vec{J}_e / e$. The rate of propagation of non-electrification in the domain is determined by the conductivity and dielectric constant. Particle difference determines the balance of created and missing particles in space dV_{DS}, $\Delta_e dV_{DS} = \left[\left(\partial n_{e.i} / \partial t\right) - divJ_e / e\right]dV_{DS}$.

6. Balances:

$\left(J_e + J_i\right)E = eV_i dn/dt + P_{izl.} - divV_i J_e - div\lambda \cdot gradT + c_p dT/dt$
, where V_i is ionization potential, λ heat dissipation coefficient, c_p thermal capacitance of the gas at constant pressure. In the left part of the equation is the power generated by the current in the domain and in the right part of the equation are the forces: 1. ionization of neutral atoms, 2. radiation, 3. expired charge carriers, 4. heat losses, 5. heating plasma.

The theory of the electric arc model is based on the definition of the arc channel, the leader and the streamer and the state is described by the equation:

$$dQ/dt = Ei_l - P_0 \quad (5)$$

where Q is amount of heat, E voltage gradient, i_l arc current, P_0 given power.

If addiction is known Q then we can determine dQ/dt. If the pressure in the arc is lower, the length of free path of electron is greater. The kinetic energy of an electron is greater than energy of positive ions and neutral particles and is determined by temperature of electron gas and not by temperature of the dielectric. The bow has three zones: K cathode, A anode and C arc pillar zone and voltage falls V_{cat}, V_{an}, $\vec{E} \cdot \vec{\ell}$. Zone proportions of A and K are les than zone C. Voltage falls V_{cat} and V_{an} créate stronger fileds E in the arc zones. For the quasi-stationary state, the volt-ampere diagram of the arc pole is:

$$v_{arc} = V_{cat} + V_{an} + E \cdot \ell \quad (6)$$

where E is potential gradient, ℓ arc length.

The arc tree is an ionized part of the gas volume whose conductivity is approximately equal to the

conductivity of the metal. The experiment shows that there is density in the arc tree $J = 5 \cdot 10^4$ [A/cm^2], gradiant $grad\varphi = -\partial E / \partial x = 15 \div 20$ [V/cm] and conductivity $\sigma = J / E$ (where $\sigma = 0.25 \cdot 10^6$ [S/m]), which is comperable with conductivity $\sigma_{Cugraph} = 0.15 \cdot 10^6$ [S/m][11].

The source of direct current arc ionization is a thermal process. Although thermal process dominates as the current passes through zero, a small impact in the shorter interval has an impact on ionization where both ionization and diffusion of ions and electrons occur. Ionization dominates when arc is ignited and deionization dominates when arc is extinguished. Arc is an electrothermal process whose simultaneous analysis is complex.

In the domain, the interaction of particles is neglected. The mean propagation velocity of electrons and ions is $\bar{v}_{me} = e\vec{E} / m\nu = b\vec{E}$. There is ion mobility in the air $b_i = 1.5 \div 2$ [cm^2/Vs] and electrons in a weak electric field $b_e = 10^3$ [cm^2/Vs] [5]. Neutral atoms and molecules are not affected by the strength of the electric field. If the ρ density of a gas is a dielectric and if they move under the influence of pressures p in the gas, then their action is described by the equations:

$$\rho(d\bar{v}_{me} / dt) = -grad(p),\ d\rho_g / dt = -\rho_g div(\bar{v}_{me}) \quad (7)$$

If charged density in the domain is sufficient to turn into an avalanche and widen the channel on both sides - toward the anode and cathode, then the discharge begins with one electron. In the Wilson chamber [5], the propagation of the channel in the field when a voltage pulse is generated between two electrodes was examined 10^{-7} [s]. The number of electrons on the forehead increased exponentially $e^{\alpha x}$ (where x is the distance of the forehead of the avalanche leader from the cathode, α is Townsend coefficient (obtained from the conditions at the head)). The largest number of positive ions is on the forehead and they, in the direction of the normal velocity, spread diffusely and spread across the cross section. The width of the avalanche in the air is 1-2 [mm], and the propagation velocity is $1.3 \cdot 10^3$ [m/s], when $E / p = 30$ [V/Pa] and $p = 30$ [kPa].

If the necessary energy for ionization of electrons is obtained by forces in an electric field, then shock ionization occurs, which is characterized by the first Townsend coefficient α_u [cm^{-1}]. It represents the number of impacts performed by electrons in an electric field at a distance of 1 [cm], according to empirical expression:

$$\alpha_y = \frac{A_0 \varphi_i p}{T} e^{-B_0 \varphi_i (T / E / p)} \text{ [cm}^{-1}\text{]} \quad (8)$$

where p is pressure, T temperature, E field strength-potential gradient φ_i , A_0 and B_0 constant.

In the part of dx streamer ℓ, in a unit of time there is n_{0-} electrons and each creates dn new electrons. On the way dx each electron provides $\alpha_y dx$ ionization and due to it $dn = \alpha_y n dx$:

$$\int_{n_0}^{n} dn = \int_0^x \alpha_y n dx \Leftrightarrow n = n_0 e^{\alpha_y x} \quad (9)$$

The number of ions formed in ionization is: $n_i = n_0 e^{\alpha_y \ell} - n_0 \Rightarrow n_i = n_0 (e^{\alpha_y \ell} - 1)$. If ions hit the cathode and new electrons erupt, the phenomenon is defined by another Townsend coefficient γ_T which defines the number of electrons that hit the cathode and emit one ion each. The discharge is self-sustaining in ionization and the formed ions that strike the cathode and erupt from it as a replacement for the number of electrons at the beginning of the process [11] are:

$$\gamma_T n_i = \gamma_T n_0 \left(e^{\alpha_i \ell} - 1\right) = n_0 \quad (10)$$

where $\gamma_T \left(e^{\alpha_i \ell} - 1\right) = 1$ is Townsend condition for self-discharge, γ_T ionization number up to $pd = 13332$ [Pam].

An electron from the cathode when moving towards the anode creates $e^{\alpha_i \ell} - 1$ of positive ions. If the voltage is $V_{p\min} \geq B(pd)_{\min}$ new channel of discharge develops. For greater electrode spacing in air (>10^2 [cm]), parts of the streamer are >10^2 [cm] and temperatures are >3000 ^{0}C. The temperature along the streamer is sufficient for thermal ionization of the air. The consequence is a higher field strength at the

head of the streamer, the development of new streamers and the extension of the primary channel due to the higher heat.

A thermally ionized main channel is then formed in an inhomogeneous electric field, a leader, with a small longitudinal electric field strength. If the leader's forehead approaches the electrode of opposite polarity, the field strength increases between the electrodes. The leader expands continuously from the anode and jumps from the negative electrode. The voltage jump in an inhomogeneous field is explained by the Pedersen semiempirical criterion.

In the plasma domain, the field strength is determined by Ohm's law $\vec{E} = \vec{j} / n_e b_e$. Inductive and electrical component $E = 10^3$ [V/cm] are comparable only for rapid current changes $\geq 10^{10}$ [A/s]. Inductivity $L \leq 1 \div 2$ [μH/m] for radius leader channels $r_S \cong 10^{-1} \div 1$ [cm] is negligable.

There is a component $\vec{E} = 0$ along the channel axis, but the field strength along the channel cross section is constant and amounts to $rot\vec{E} = 0$. Due to the conductive structure of the leader, there is also a longitudinal capacitance of the channel, which in the final conductivity is not filled and not emptied currently. The longitudinal value of the current is not the same and there are leads:

$$\frac{\partial i(x,t)}{\partial x} = -\frac{\partial q(x,t)}{\partial t} \tag{11}$$

where $q(x,t)$ is the amount of electrification (load).

The following equation should be solved when calculating the field strength in the plasma domain:

$$div\vec{E} = \rho_e / \varepsilon,\ divgrad(v_{V=\varphi}) = \rho_e / \varepsilon \tag{12}$$

where v is the field potential, ρ_e volumetric density of the load.

Boundary conditions are a potential at the electrodes and the outer surface of the leader channel, but due to the complex boundary geometry, it is difficult to make a model for field calculation outside the channel domain. The voltage at the leader's head does not depend on electrode spacing for constant charges and thus a calculation for each step is avoided. The solution of electrothermal processes in gas is complex because, due to different process speeds, it is difficult to determine the integration step. If it is chosen according to the criterion of fast processes, the number of steps in time increases infinitely, and if it is chosen according to criterion of slow processes, the errors are large. According to the criterion of propagation speed, processes are divided into 3 groups: the fastest processes with time 10^{-9} [s] - establishment of electron distribution function and their temperature, medium-fast processes with time 10^{-7} [s] - processes that change the concentrations of loaded and excited particles, and slow processes over time 10^{-7} [s] - gas heating and ambipolar (multipolar) diffusion. The division enables analysis of formation and disappearance of electrons in context of establishing a quasi-stationary value of electron gas temperature and the gas temperature that remains unchanged.

Potential-voltage $v(x,t)$ and current $i(x,t)$ per intersection at a point x are:

$$\frac{\partial v(x,t)}{\partial x} = -E(x,t) - \frac{i(x,t)}{G(x,t)},$$
$$\frac{\partial i(x,t)}{\partial x} = -\frac{\partial q(x,t)}{\partial t} \tag{13}$$

where $G(x,t)$ and $q(x,t)$ are drainage-conductivity and load unit length leader.

The presence of electrodes affects distribution of charge along the leader because it is determined by the capacitance and potential of the streamer. At front of the arc towards anode on streamer casing is the surface density $\eta = q / S_{out}$ (cilindre $S_{out} = 2\pi r_l \ell_l$) and electrification $q = c\grave{v}(x = l, t)$. The effective potential in the channel axis is voltage difference $\varphi(x,t) = V(x,t) - V_e(x,t)$ (actual voltage $V(x,t)$ and voltage $V_e(x,t) \approx V_{a.k}$ electrodes). When there are no electrodes, size $\varphi(x,t)$ corresponds to the true value of the potential at a given point.

If the potential $\varphi(x,t)$ proportional to the charge of the electrodes, the field is shaped by the charges at the top and the streamers in front of the top of the leader. Potential $\varphi(x,t)$ points $x = x_V = \ell$ it is equal to the potential of the top

leader. At the point $M(x,y)$ potential value $\varphi(x,t)$ on the surface of the streamer is the sum of the potentials of the streamer, the longitudinal charge density $q(x,t)$ and the potential of the distributed charges on the electrode surfaces, $\eta(x,t)$:

$$\varphi(x,t)=\int_0^{\ell}\frac{q(y,t)}{4\pi\varepsilon|y-x|}dy+\int_S\frac{\eta(M,t)}{4\pi\varepsilon\cdot r_{Mx}}dS \quad (14)$$

By separating part of the potential-voltage generated by the charge of the streamer at point x the coordinate of the potentials of other charges generated at the same point x it is in the interspace:

$$V(x,t)=\frac{q(x,t)}{C(x,\ell)}+V_{out}(x,t) \quad (15)$$

where $C(x,\ell)$ is longitudinal capacitance of the streamer depending on the point coordinate $M(x,y)$ and channel lengths ℓ.

Potential part $V_{out}(x,t)$ of total potential $V(x,t)$ when they create electrodes, the electrode is significantly larger than the part of the potential of the streamer, i.e. it's about:

$$V_{out}(x,t)\approx V_{el}(x,t)=\int\frac{\eta(M,t)}{4\pi\varepsilon\cdot r_{Mx}}dS \quad (16)$$

For $C(x,\ell)$ potential

$\frac{q(x,t)}{C(x,t)}=\varphi(x,t)=V(x,t)-V_{el}(x,t)$ defines electrification of strimer.

The charge of the streamer sheath depends on the charge of the electrodes that form the channel and does not depend on the potential of the point. If they are evenly spaced along the leader axis, $C(x,\ell)$ is determined per Lama method [12]:

$$\varphi\approx V=\frac{Q}{4\pi\varepsilon}\left[\int_0^{\ell-x}\frac{dx}{\sqrt{x^2+r_s^2}}+\int_0^{-x}\frac{dx}{\sqrt{x^2+r_s^2}}\right]=\frac{Q}{4\pi\varepsilon}\left[\ln\frac{\left(\ell-x+\sqrt{(\ell-x)^2+r_s^2}\right)\left(x+\sqrt{x^2-r_s^2}\right)}{r_s^2}\right] \quad (17)$$

The equation of effective potential in the domain is:

$$\frac{\partial^2\varphi(x,t)}{\partial x^2}+a(x,t)\frac{\partial\varphi(x,t)}{\partial x}-b(x,t)\frac{\partial\varphi(x,t)}{\partial t}=F(x,t) \quad (18)$$

where $a(x,t)=\frac{1}{G(x,t)}\frac{\partial G(x,t)}{\partial x}$, $b(x,t)=\frac{C'(x,t)}{G(x,t)}$, $F(x,t)=\frac{E_e(x,t)}{G(x,t)}\cdot\frac{\partial G(x,t)}{\partial x}+\frac{\partial E_e(x,t)}{\partial x}$.

Boundary conditions for the equation (18) (anode $\varphi=0$) they are at the top of the leaders:

$-\frac{\partial\varphi}{\partial x}=\frac{C_{fr.lead}\bar{v}_s\varphi_s}{b_e n_e e\pi\cdot r_s^2}$ and $_s=V_{an.cat}$.

For the solution, it is necessary to know the concentration of charge during the formation of the streamer at the point when gas temperature is equal to ambient temperature. As the channel expands and extends, the domain boundary changes by $d\ell/dt=\bar{v}_s(\varphi_s)$ and for a given value $\rho\ r_s^2\pi=C^{ta}$:

a) channel radius r_s [m] increases due to thermal expansion (continuity equation for gas molecules) or

b) $d\left(r_s^2\right)/dt=4D_a$ if due to diffusion the channel expands.

Experiments show that the radius of the avalanche $r_s\approx10^{-4}$ [m], $n_e\approx10^{12}\div10^{13}$, $\ell\approx10^{-5}$ [m] and for $r_s\gg\ell$ gas in transitions to an electric arc.

If the boundary conditions are met, the field strength in the channel can be determined by the equation:

$$E(x,t)=-\frac{\partial V(x,t)}{\partial x}=-\frac{\partial(x,t)}{\partial x}+E_e(x,t)=\frac{C_{fr.lead}\bar{v}_s{}_s}{b_e n_e e\pi\cdot r_s^2}+\frac{V_{an.cat}}{\ell}=\frac{4\pi\varepsilon}{\ln(\ell/r_s)}\frac{\bar{v}_s{}_s}{b_e n_e r_s^2\pi}+\frac{V_{an.cat}}{\ell} \quad (19)$$

The field strength distribution around the streamer face depends little on the length of the streamer and is best suited to the field distribution around the sphere with the potential of the streamer head:

$$\vec{E}=\frac{q}{4\pi\varepsilon\cdot r^2},\ r\ge a_{sf},\ \vec{E}=\frac{q}{4\pi\varepsilon\cdot a^2},\ r=a_{sf},\ \vec{E}=\frac{q}{4\pi\varepsilon\cdot a^3}\vec{r},\ r<a_{sf} \quad (20)$$

The field strength next to the streamer front is:

$$\frac{dE_x}{dx} = -\frac{E(x)}{x} - \frac{n_+ - n_e - n_-}{\varepsilon} e\Big|_{n_e = n_+ = n_{e.front}} \quad (21)$$

An expression for potential is added to the equation for the process around the streamer's forehead $\varphi_s = \int_{r_{fr}}^{\infty} E(x)dx$ and the continuity condition (conduction current behind the streamer front $J_{behind\ .fr} = (\partial D / \partial t)_{ahead\ .fr}$ equal to the dielectric displacement current in front of the streamer front $n_{e.fr} b_e e E_{fr} \pi \cdot r_{fr}^2 = C\bar{v}_{st.}\varphi_s$).

Equality is enough for an approximate solution $\varphi_s = V_{an.cat}$ and data on pressure, temperature, humidity and anode-cathode voltage field strength in the streamer direction. The arc voltage has three components: in the cathode domain V_c, anode V_a and the length of the arch pillar ℓ_l:

$$v_\ell = V_c + V_a + V_{s\ell} = V_c + V_a + grad\varphi_{,\varphi=V,\ell=\ell} \quad (22)$$

The wiring diagram includes the parameters of important elements. Circuit parameters can be concentrated and distributed. For voltage calculation u_p two methods are used, namely: the method of contour currents and the method of superposition.

The first method starts from Kirchhoff's rules. For a potential circuit scheme in the event of a power failure and the appearance of an arc, a sufficient number of equations for contours are compiled, then the unknowns are excluded and one differential equation is kept in which one unknown is solved (voltage u_p), which depends on parameters and times (argument). The equation is:

$$u^n{}_p / dt^n + a_1 d^{n-1} u_p / dt^{n-1} + ...a_n u_p = f(t) \quad (23)$$

The solution of this equation consists of two components $u_p(t) = u_{forc}(t) + u_{free}(t)$.

Forced component $u_{forc}(t)$ is a partial solution of the inhomogeneous differential equation for the stationary mode in the circuit, i.e. the source voltage, ie. at the time of voltage establishment after the current has passed through the zero value. Free component $u_{free}(t)$ is general solution:

$$u_{forc}(t) = A_1 e^{r1t} + A_2 e^{r2t} + ...A_n e^{rnt} \quad (24)$$

where $A_1 - A_n$ are constants, $r_1 - r_n$ the roots of the characteristic equation corresponding to the equation (23).

During the transition from the time domain to the complex domain, the initial conditions are taken into account and no integration constants are required, because at the beginning a system of equations in the operator form was compiled. Transformations of unknowns are excluded from the system of equations and only the transformation of the required quantity remains $u_{forc}(p) \Leftrightarrow u_p(t)$ in the form: $u_{forcp}(p) = A_1(p) / A_2(p)$.

In the superposition method, the process of current interruption in a switch with an arc is equivalent to the inclusion in the circuit of a conditional source with a current equal in intensity and opposite in direction to the tripping current (the resulting current is equal to zero) [17,18]. Combined with the operator this method allows the setting voltage to be determined with:

$$U_p(p) = I(p) \cdot Z(p) \quad (25)$$

where $I(p)$ and $Z(p)$ operator form of current and impedance of a circuit reduced at a short-circuited power supply.

Due to the small value of the inductance of the arc, the active part of the impedance of the arc has a nonlinear character. Value u_p after the passage of current through zero heavier values U_0. Before it reaches zero, the arc resistance R_l switches increase significantly, so does the arc voltage U_l. The arc current i_l decreases compared to the conditions when it was $R_l = 0$ and $U_l = 0$. There are also experimental methods for measuring values u_p. The voltage establishment process, depending on the relationship of the contour parameters, has a periodic or aperiodic character.

4. INFLUENCE OF ELECTRIC ARC ON ESTABLISHED VOLTAGE IN A CIRCUIT WITH ONE FREQUENCY

The established voltage with the frequency of the source in RLC the circuit in Fig. 1 is:

$$u_p = \sqrt{2} U_f k_{sh} \sin(\omega t + \varphi) \quad (26)$$

where U_f is phase voltage of the source, φ phase position between current and voltage.

Changing the voltage at the arc leads to the occurrence of current through the capacitance:

$$i_C = C(du_C / dt),\ u_C = u_l = u_p \quad (27)$$

$$u_0(t) = iR + L\frac{di}{dt} + u_p,\ i = i_{arc} + i_s,$$

$$i_C = C\frac{du_p}{dt},\ i_l = \frac{u_p}{R_{arc}},\ i_s = \frac{u_p}{R_s} \quad (28)$$

The nonlinear volt-ampere characteristic of an arc pole has three exponential functions for the reference current (0.5 or 1 [kA]): segment $1K$ and parameter of segment α_1, segment $2K$ and parameter of segment α_2 and segment $3K$ and parameter segment α_3, Fig. 1 and is:

$$U / U_{ref} = K_i (I / I_{ref})^{1/\alpha_i} \quad (29)$$

For source voltage u_0, the role of resistance on the source side R it is not large and can therefore be neglected:

$$LC\frac{d^2u_p}{dt^2} + \left(\frac{L}{R_s} + \frac{L}{R_{arc}}\right)\frac{du_p}{dt} + \left(1 - \frac{L}{R_{arc}^2}\frac{dR_{arc}}{dt}\right)u_p = u_0(t) \quad (30)$$

where u_0 is source voltage, R and L active and inductive resistance of the side of source, R_{arc} and C_{arc} nonlinear resistance and capacitance of the arc in the switch P.

Table 1. Equivalent arc resistance (active character)

Equations	Schier	Burgsdorf	Warington
R_{arc} [Ω]	$R_{arc} = 370 \cdot \ell_{arc} / I_{arc}^{0.87}$	$R_{arc} = 1.05 \cdot \ell_{arc} / I_{arc}$	$R_{arc} = 8750 \cdot \ell / I^{1.4}$
Value	ℓ_{arc} [m]	I_{arc} [A], $I \geq 10^2$ [A]	$E \approx 15 \div 20$ [V/cm]

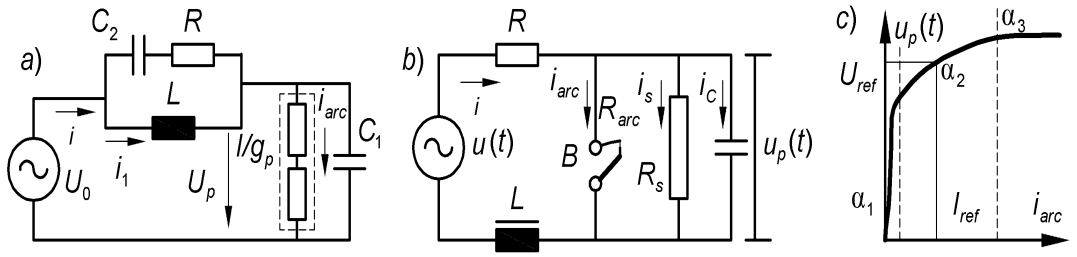

Fig. 1. Single-frequency electric circuit in which the action of the arc is analyzed and the establishment of voltage at the switch contacts: a) classical circuit diagram, b) new circuit diagram, c) nonlinear resistance of the electric arc

For easier integration, the right-hand side of the equation is multiplied by a coefficient LC and with another excerpt u_p an equation is obtained:

$$A\frac{d^2x}{dt^2} + B\frac{dx}{dt} + Cx = A \cdot f(t) \quad (31)$$

The obtained equation is translated as a characteristic equation $Ar^2 + Br + C = 0$ whose solutions

$$r_{1,2} = k_{1,2} = -\frac{B}{2A} \pm \sqrt{\frac{B^2}{4A^2} - \frac{C}{A}} = -a \pm m.$$

If C_1 and C_2 are integration constants, then is the solution of the equation (31):

$$x = e^{-at}\left\{C_1 e^{-mt} + C_2 e^{mt} + \frac{1}{2m}\left(e^{mt}\int e^{-k1 \cdot t} f(t)dt - e^{-mt}\int e^{-k2 \cdot t} f(t)dt\right)\right\} \quad (32)$$

With help of equation (32) and equation (30) can be sovled with conditions $u_0(t)=U_0=const.$, $R_l=\infty$, $dR_l/dt=0$ and it gets:

$$\frac{d^2u_p}{dt^2}+\left(\frac{1}{C_{arc}R_s}\right)\frac{du_p}{dt}+\frac{u_p}{LC_{arc}}=\frac{U_0}{LC_{arc}} \quad (33)$$

With initial conditions $t=0$, $u_p=0$ and $du_p/dt=0$ it gets:

$$u_p=U_0\left[1-\left(\frac{a}{m}shmt+chmt\right)e^{-at}\right] \quad (34)$$

where $a=\frac{1}{2C_{arc}R_s}$, $m=\sqrt{\frac{1}{4C_{arc}^2R_s^2}-\frac{1}{LC_{arc}}}$.

In equation (34) m represents an imaginary and hyperbolic function that turns into an ordinary trigonometric function and the process of establishing voltage has a periodic character (curve 2 in Fig. 2).

The aperiodic character arises from inequality $R_s<(1/2)\sqrt{L/C_{arc}}$ (curve 1 on Fig. 2).

If inequality is met $\frac{1}{2C_{arc}^2R_s^2}<\frac{1}{2LC_{arc}}$ then $R_s>\frac{1}{2}\sqrt{\frac{L}{C_{arc}}}$.

The transition from the aperiodic to the periodic process can be achieved by changing the active resistance R_s.

5. SIMULATION MODEL, SIMULATION DIAGRAMS AND RESULTS

The performed analytical considerations show the functional possibilities of the electric arc process model in the circuit breaker.

As this is a new method based on application of artificial intelligence in high voltage technology, no similar approach was found in the accessible references that would allow comparative analysis. As stated in references [2,5,6] there is a certain resemblance to the theoretical part, but in practical terms it does not exist, so this paper can be considered special because of its ability to replace expensive and complex experiments.

The system of previously derived equations is easily implemented in blocks offered by the MATLAB Simulink software package [19]. The model compiled for the MATLAB Simulink software package allows to simulate the transient processes of electrical circuits in which an electric arc occurs.

The presented method and simulation enable fast and quality solving of processes that are important for electrical equipment. Using experiences in process simulation in a single-phase electric circuit with the appearance of an electric arc during circuit switching, voltage and frequency values can be evaluated.

The parameters of the scheme elements are given in Fig. 3 (line-SCOPY1, SCOPY2), and simulation current and voltage diagrams in Fig. 4 (a,b).

An adapted program in the MATLAB psbnewarc.mdl software package with the following parameters was used to verify the model and algorithm:

- Source 35 [kV], 50 [Hz], impedance Power System: $R_1=1$ [Ω], $L_1=3.5e-3$ [H], $R_2=30$ [Ω], $L_2=5.2e-3$ [H], $C_2=1.9e-9$ [F],

- Block parameters Arc in a Breaker:

$g=1e4$ [S], $R_{arc}=1.e-4$ [Ω], $C_{arc}=1.98e-9$ [F], $R_{shant}=f(V,I)$,

-**Block parameter VA characteristic in arc:**

$V_{ref}=35.0e3$ [V], $I_{ref}=1$ [kA], $Seg.ch.=0.955$, $k_1=50$, $\alpha_1=1.0$, $k_2=0.25$, $\alpha_2=0.99$, $k_3=16.5$, $\alpha_3=0.98$,

- **Load parameters:**

$V_n=35e3$ [V], $f=50$ [Hz], $L=6.2e-4$ [H], $R=450$ [Ω].

An adapted part of the MATLAB Simulink software package was used to determine the voltage diagram. The shapes that indicate overvoltages on the switch are shown in Fig. 4.(a,b). This means that before measuring the overvoltage on the circuit breaker contacts, according to the described method, their values as well as their time course can be estimated. From the diagram in Fig. 4.(a,b) concludes how the process took place at each time point (comparative diagrams of currents and voltages are shown: models of M. Kassi and O. Mayr and a new theoretical model of an electric arc).

The process simulation. Although the natural frequency is set f_0, the capacitance of the arc is important for the appearance of the arc in the circuit C_{arc} which is often not known. If inductance is known L (and other parameters), capacitance C_{arc} can be determined from the frequency f_0 or by applying some of the derived equations. By switching off the capacitance C_{arc} conditions can be obtained for the transition from periodic to aperiodic process in which voltage will be established u_p.

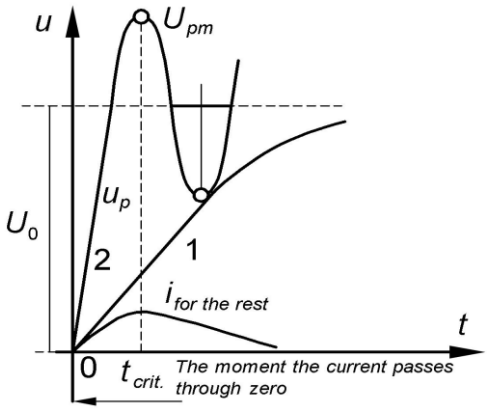

Fig. 2. Diagram u_p in periodical (curve 2) and aperiodical process (curve 1)

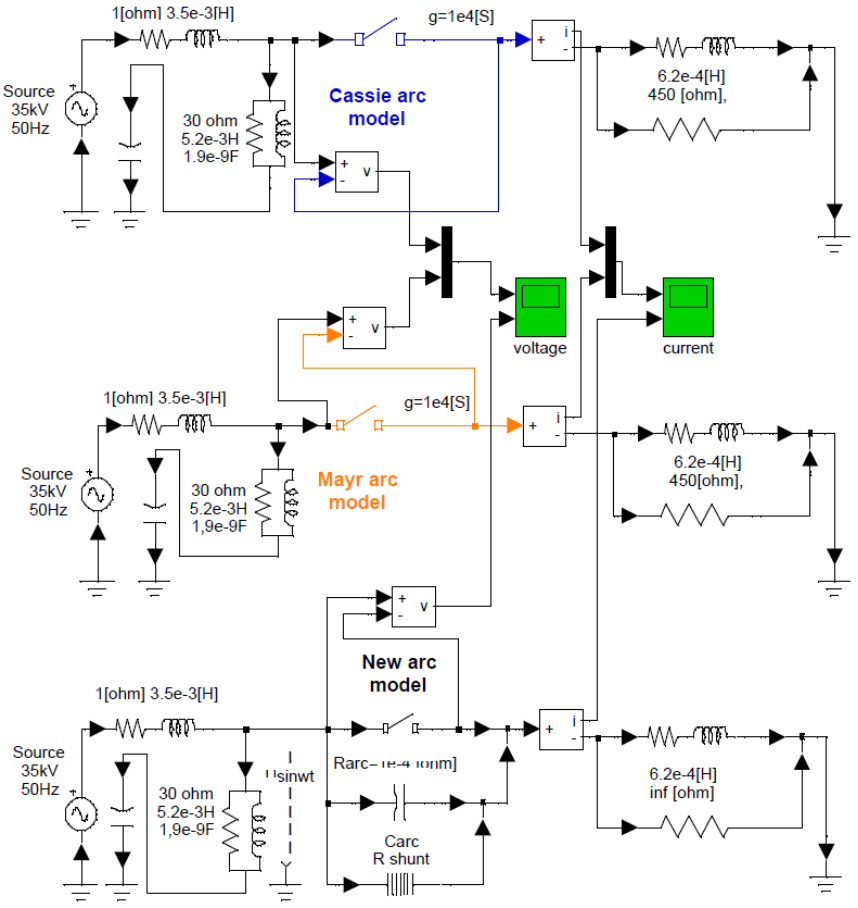

Fig. 3. Model scheme for simulation of transient process in arc in circuit breaker

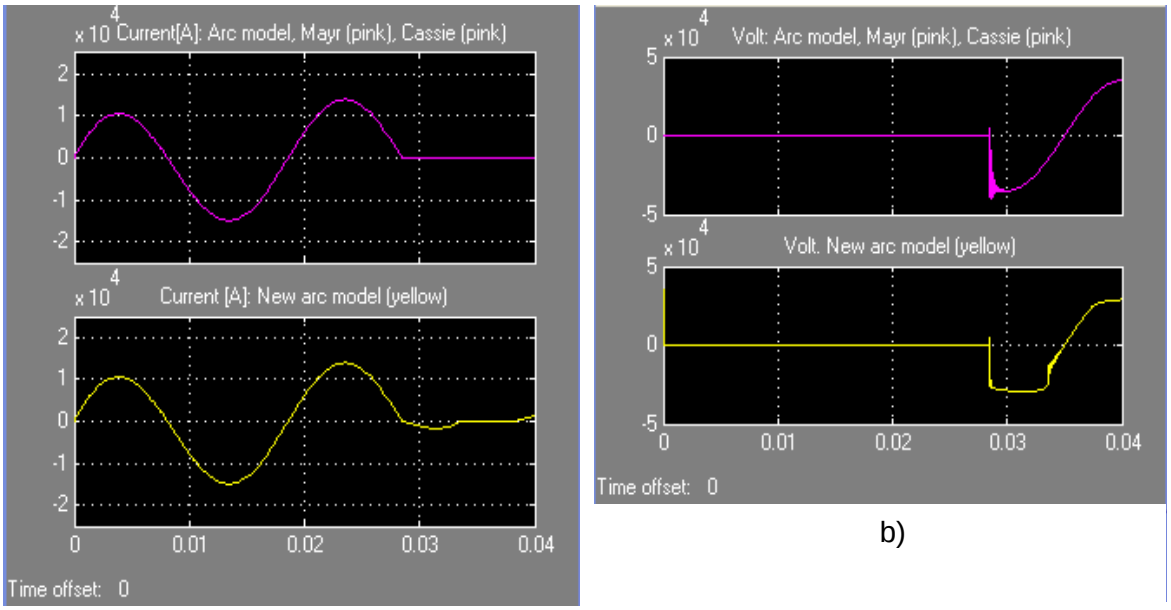

a) b)

Fig. 4. Comparison of diagram of a) current and b) voltage of arc in the Breaker

From the functions and diagrams obtained by the simulation, the influence of the parameters of the circuit elements on the voltage is obvious u_p. Capacitance present C_{arc} is loaded from the source through inductance L and resistance R which dampens the process, absorbs some of the energy and converts it into losses. If capacitance C_{arc} increases, the voltage can be lower and the speed of voltage establishment is lower u_p. Resistance R_{shant} in parallel branch, on switch or residual resistance of arc column serves for partial discharge of static charge from arc capacitance C_{arc} and thus reduces the rate of voltage establishment.

On the one hand, an increase in inductance L slows down the capacitance load C_{arc} and reduces the rate of voltage establishment, but on the other hand leads to an increase in the phase position between currents and voltages, which also means an increase U_0, i.e. to an increase in the absolute value and the rate of voltage establishment u_p. For higher circuit natural frequencies, residual resistances have a greater impact on process damping during the first curve domain u_p since by that time it is not yet great. If the trip circuit has a low natural frequency of the circuit, the residual resistances also affect the shape of the set-up voltage u_p.

The active resistance in the electrical circuit dampens the oscillations, but does not affect their character. To the obtained result, if it is of interest for obtaining exact values, a function related to oscillation damping can be added.

6. CONCLUSION

In order to check the previously performed equations of the electric arc in the switch, a simulation was performed in the part of the software package MATLAB Simulink called psbnewarc.mdl, Fig. 3 (according to the developed mathematical model in parts 3 and 4). The obtained diagrams, Fig. 4 (a,b), confirm that the derived relations are in accordance with the given values in the simulation model.

A basic analytical model is required to create a process model in an arc circuit. Analytically derived equations with simple conditions and assumptions, although they introduce certain inaccuracies, provide a very objective picture of the process. The model is adapted to new tendencies and knowledge based on the application of artificial intelligence, and obtained result is a special model that presents real processes. Theoretical model of work included important influences, and derived current and voltage equations were successfully introduced into the software part of package for simulation and to obtain approximately accurate results of modeling process of arc interruption.

MATLAB Simulink programs simulate electrical circuits where an electric arc occurs quite accurately, but their own development of both models and programs has special advantages such as detailed insight into all components of models and programs and making various changes that would not otherwise be possible in available software packages.

The advantage of the simulation in relation to the practical model (experiment) is that it is completely safe for the drive system and personnel, and the obtained results agree very well with the real situation and processes.

In order for the work not to be too extensive in some of the following works, new results related to additional simulations with a larger number of parameters that affect the processes in the electric arc will be presented.

COMPETING INTERESTS

Authors have declared that no competing interests exist.

REFERENCES

1. Habedank U. On the Mathematical Description of Arc Behaviour in the Vicinity of Current Zero. etzArchiv. 1988; 10(11):339-343.
2. Yuan L, Sun L, Wu H. Simulation of Fault Arc Using Conventional Arc Models. Energy and Power Engineering. 2013; 05(04):833-837.
   Available:https://www.researchgate.net/publication/274123237_Simulation_of_Fault_Arc_Using_Conventional_Arc_Models
3. Bjelić SN, Marković FN, Marković NA. Transient Process at Atmospheric Discharge into the Landline and the Appearance of an Electric Arc in the Switch. International Journal of Information Technology and Computer Science (IJITCS). 2021;13(2):27-37.
   Available:http://www.mecs-press.org/ijitcs/ijitcs-v13-n2/IJITCS-V13-N2-3.pdf
4. Bjelić SN. Atmospheric and commutation overvoltages in electrical distribution networks. Kraljevo: Kvark; 2020.
5. Cassie AM. Theorie Nouvelle des Arcs de Rupture et de la Rigidité des Circuits. CIGRE. 1939;102:588-608.
6. Mayr O. Beitrage zur Theorie des Statischen und des Dynamischen Lichtbogens. Archiv für Elektrotechnik. 1943;37(12):588-608.
7. Schavemaker PH, Van der Sluis L. An Improved Mayr-Type Arc Model Based on Current-Zero Measurements. IEEE Transactions on Power Delivery. April 2000;15(2):580-584.
   Available:https://ieeexplore.ieee.org/document/852988
8. Marković N, Bjelić S, Živanić J, Jakšić U. Numerical simulation and analytical model of electrical arc impedance in the transient processes. Przeglad Elektrotechniczny. January 2013;89(2): 113-117.
   Available:https://www.researchgate.net/publication/287082140_Numerical_simulation_and_analytical_model_of_electrical_arc_impedance_in_the_transient_processes
9. Bron OB. Potoki Plazme v električeskoi dugi viklucajesciech apparatovi. Enegija. Leningrad; 1975.
10. Bazeljan EM. Razanski IM. Iskrovoi razrjad v vozduhe. Sibirskoe Otdelenie Akademii nauk SSSR. Novosibirsk: Nauka; 1998.
11. Bronštein IN. Semendjajev KA. Spravočnik po matematike dja inžinjerov i... Mir. FM: Moskva; 1982.
12. Zalesskij AM. Električeskaja duga otlkločenija. Gosenergoizdat. Moskva; 1963.
13. Levinštejn ML. Operatorovy počet v elektrotechnice. SNTL Praha; 1977.
14. Schier A. Resistance of electrical arc in very high voltage networks. Elect. India. 1970;8:5-9.
15. Burgsdorf VV. Otkritie elektriceskie dugi bolsoi mosnostei. Elektricestvo. 1948;10: 15-23.
16. Van AR. Warington C. Protective relay. Theory and Practice. New York: Champan & Hill; 1994.
17. Jakšić U, Marković N, Živanić J, Milenković N. Development of the Model for Simulation of Transient Processes in Cables and Power Lines. Original Research Article. February 2018;25(6): 1-10.
   Available:https://www.journalcjast.com/index.php/CJAST/article/view/9696
18. Van der Sluis L, Rutgers WR, Koreman, CGA. A physical arc model for the simulation of current zero behaviour of high-voltage circuit breakers. IEEE

Transactions on Power Delivery. 1992; 7(2):1016-1022.
Available:https://ieeexplore.ieee.org/document/127112

19. MATLAB Simulink SimPowerSystem. Copyright 2002 TheMathWorks. Version 6.5.0,180913a.

Peer-review history:
The peer review history for this paper can be accessed here:
https://www.sdiarticle4.com/review-history/74830